



Polynuclear nickel(II) complexes with salicylaldehyde derivative ligands

Moussa Dieng^a, Ousmane Diouf^a, Mohamed Gaye^{a,*}, Abdou Salam Sall^a, Paulo Pérez-Lourido^{b,*}, Laura Valencia^b, Andrea Caneschi^c, Lorenzo Sorace^c

^a Department of Chemistry, University Cheikh Anta Diop, Dakar, Senegal

^b Departamento de Química Inorgánica, Facultad de Química, Universidad de Vigo, 36310 Vigo, Pontevedra, Spain

^c Dipartimento di Chimica "U. Schiff" and INSTM Research Unit, Università di Firenze, Via della Lastruccia 3, 50019 Sesto Fiorentino, FI, Italy

ARTICLE INFO

Article history:

Received 23 April 2012

Received in revised form 26 September 2012

Accepted 26 September 2012

Available online 12 October 2012

Keywords:

Nickel

Polynuclear

Salicylaldehyde

Antiferromagnetic

ABSTRACT

The reaction of pentadentate salicylaldehyde ligand 2-((2-(2-(2-hydroxybenzylideneamino)ethylthio)ethylimino)methyl)phenol (**H₂L**) and its related hydrogenated derivative 2-((2-(2-(2-hydroxybenzylamino)ethylthio)ethylamino)methyl)phenol (**H₄L¹**) with hydrated nitrate and perchlorate nickel(II) salts afforded polynuclear metal complexes. These complexes were characterized by elemental analysis, IR and UV–Vis spectroscopy, molar conductance and variable temperature magnetic measurements. Single crystal X-ray diffraction of $[(\text{NiL})_2] \cdot \text{CH}_3\text{OH} \cdot 4\text{H}_2\text{O}$ (**1**) and $[\text{Ni}_3(\text{H}_2\text{L}^1)_2(\text{NO}_3)_2]$ (**3**) complexes has revealed the presence of an octahedral coordination geometry around the nickel ion. The magnetic data indicate that a moderate antiferromagnetic interaction is present in complexes **1** and **3**.

© 2012 Elsevier B.V. All rights reserved.

1. Introduction

Studies involving the chelation and coordination of ligands derived from salicylaldehyde to transition metal centers containing a flexible tridentate ligand have been an ongoing area of active research. In recent years, much attention has been given to the synthesis of acyclic ligands that can give rise to dinuclear or polynuclear metal complexes with interactions between the metal centers [1,2]. Salicylaldehyde has been used as precursor of a high number of acyclic ligands with several different donor sites using different amines [3–5]. The formation of acyclic complexes depends on the dimension of the cavities, on the flexibility of the arms, on the nature of the donor atoms and on the complexing properties of the anions acting as counter ions [6]. Attention has been devoted to the study of spectroscopic properties and crystal structures [7,8].

Some metalloproteins contain metal ions such as Ni(II) or Cu(II) where the coordination spheres present N and S donor sets. These features have led to increased interest in the synthesis of complexes with mixed N,S donating chelates as structural models of the active sites [9,10]. In this paper, we report our work with acyclic ligands derived from the salicylaldehyde precursor and 2-(2-aminoethylthio)ethanamine. In this case, we have prepared the acyclic **H₂L** and its related hydrogenated derivative **H₄L¹** ligands

(Scheme 1), which have large receptor cavities with N and S donor sites suitably disposed to encapsulate one or more metal ions, resulting in di- or trinuclear complexes. The complexation capacity of these acyclic ligands towards the first row transitional metal Ni(II) ion has been investigated.

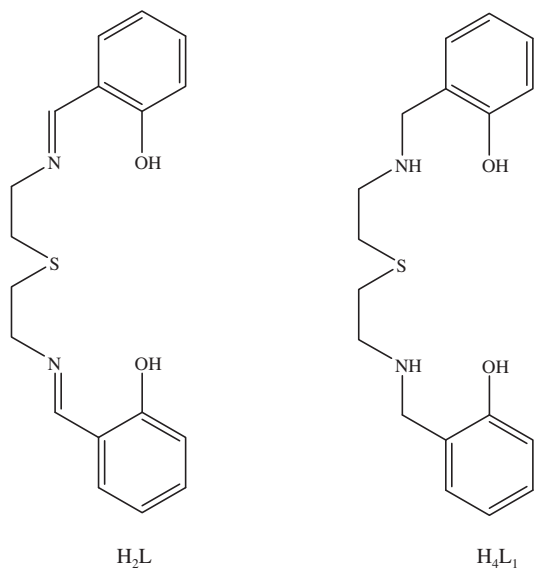
2. Experimental

2.1. Physical measurements

Elemental analyses were carried out using a LECO CHNS-932 instrument. The IR spectra were recorded as KBr discs on a Bruker IFS-66 V spectrophotometer (4000 to 400 cm^{-1}). The UV–Vis spectra were run on a Shimadzu UV-2501 PC Recording Spectrophotometer (1000 to 200 nm). The FAB mass spectra were recorded using a Micromass Autospec spectrometer using 3-nitrobenzyl alcohol as the matrix. The ¹H and ¹³C NMR spectra of the Schiff bases were recorded in CDCl₃ on a BRUKER 500 MHz spectrometer at room temperature using TMS as an internal reference. The molar conductance of 10^{−3} M solutions of the metal complexes in DMF was measured at 25 °C using a WTW LF-330 conductivity meter with a WTW conductivity cell. Magnetic measurements were performed in the temperature range of 2–300 K by using a Cryogenic S600 SQUID magnetometer in an applied magnetic field of 1000 Oe. Raw data were corrected for the diamagnetism of the sample holder, measured in the same temperature and field range, and the intrinsic contribution of the sample, estimated by Pascal's constants.

* Corresponding authors.

E-mail addresses: mlgayeastou@yahoo.fr (M. Gaye), paulo@uvigo.es (P. Pérez-Lourido).



Scheme 1.

2.2. Chemicals and starting materials

2-(2-Aminoethylthio)ethanamine, salicylaldehyde, sodium tetrahydroborate and hydrated nitrate and perchlorate salts Ni(II) salts were commercial products (from Alfa and Aldrich) and were used without further purification. Solvents were of reagent grade and were purified by the usual methods.

Caution: Although no problems were encountered during the course of this work, attention is drawn to the potentially explosive nature of the perchlorate salts.

2.3. Synthesis of the ligands

2.3.1. H_2L

2-(2-Aminoethylthio)ethanamine (4.17 g, 34.7 mmol) dissolved in 30 mL of ethanol was refluxed with an ethanolic solution of salicylaldehyde (8.47 g, 69.4 mmol), in the presence of few drops of glacial acetic acid [11]. The resulting yellow solution was refluxed for 3 h. On cooling to room temperature a separated yellow precipitate was formed. It was thoroughly washed with ether and dried over P_4O_{10} . *Anal. Calc.* for $C_{18}H_{20}N_2O_2S$: C, 65.8; H, 6.1; N, 8.5; S, 9.8. *Found:* C, 65.5; H, 6.1; N, 8.5; S, 9.9%. *Yield:* 87.4%. *M.P.:* 75 °C. *MS (FAB, m/z):* 329 [H_2L] $^+$. *IR (KBr, cm^{-1}):* 3354s (ν_{O-H}); 3135m, 3052m, 1149s, 1069m, 955s, 891s (ν_{CH}); 2854s (ν_{CH_2}); 1633s ($\nu_{C=N}$); 1577s, 1526w, 1418s ($\nu_{C=C}$); 1244m (ν_{C-O}). 1H NMR ($CDCl_3$) δ 2.9 (t, 4H, $-CH_2-S-$), 3.8 (t, 4H, $-CH_2-N=$), 8.4 (s, 2H, $HC=N-$), 6.8–7.4 (m, 8H, H_{Ar}), 12.25 (s (broad), 2H, $-OH$) ppm. ^{13}C NMR ($CDCl_3$) δ 166.06 ($-C=N-$), 161.04, 132.41, 132.25, 131.49, 118.69, 117.03 (C_{Ar}), 59.40 ($-CH_2-N-$), 33.45 ($-CH_2-S-$) ppm.

2.3.2. H_4L^1

H_2L (5.08 g, 15.5 mmol) was dissolved at 0 °C in 70 mL of methanol and (1.76 g, 46.4 mmol) of $NaBH_4$ was added in small portions [12]. The white precipitate which was formed during the reaction was isolated by filtration. The solid product was washed with several portions of diethylether and dried in a vacuum dessicator over P_4O_{10} . *Anal. Calc.* for $C_{18}H_{24}N_2O_2S$: C, 65.0; H, 7.3; N, 8.4; S, 9.6. *Found:* C, 65.1; H, 7.3; N, 8.4; S, 9.7%. *Yield:* 97%. *M.P.:* 103 °C. *MS (FAB, m/z):* 333 [H_4L^1] $^+$. *IR (KBr, cm^{-1}):* 3354s (ν_{O-H}); 3277m, 3038m, 1082s, 983s, 870s (ν_{CH}); 2833s (ν_{CH_2}); 1577s, 1526w, 1461s, 752s ($\nu_{C=C}$); 1278m (ν_{C-O}). 1H NMR $CDCl_3$ δ 2.9 (t, 4H,

$-CH_2-S-$), 3.8 (t, 4H, $-CH_2-N-$), 4.9 (s, 2H, $HN-$), 3.8 (t, 4H, $Ar-CH_2-N-$), 6.8–7.4 (m, 8H, H_{Ar}), 12.25 (s, (broad), 2H, $-OH$) ppm. ^{13}C NMR ($CDCl_3$) δ 158.07, 128.87, 128.42, 122.19, 119.16, 116.46 (C_{Ar}), 52.20 ($-CH_2-N$), 46.84 ($Ar-CH_2-N-$), 31.81 ($-CH_2-S-$) ppm.

2.4. Synthesis of the complexes – General procedure

To a refluxing methanolic solution (10–20 mL) of the perchlorate or nitrate metal salt (2 mmol), a solution of the corresponding ligand (1 mmol) in methanol (15–30 mL) was slowly added. The solution was stirred at room temperature for 2 h and then let stand to cool. The precipitate obtained was isolated by vacuum filtration, washed with cold methanol and dried over anhydrous P_4O_{10} . In the case of complexes **1** and **3**, no precipitate from the mixture solution was formed, thus the resultant green solutions were filtered. Crystals of $[(NiL)_2] \cdot CH_3OH \cdot 2H_2O$ (**1**) and $[Ni_3(H_2L^1)_2(NO_3)_2]$ (**3**), were obtained by slow evaporation of the green solution after 3 days.

2.4.1. $[(NiL)_2] \cdot CH_3OH \cdot 4H_2O$ (**1**)

Anal. Calc. for $C_{37}H_{44}Ni_2N_4O_7S_2$: C, 53.0; H, 5.3; N, 6.7; S, 7.6. *Found:* C, 53.0; H, 5.3; N, 6.6; S, 7.6%. *Yield:* 39%. *IR (KBr, cm^{-1}):* 3489m, 3024w, 2911m, 2858m, 1627s, 1595s, 1547s, 1469m, 1289s, 1100m, 894m, 788m, 759s, 592m. $A_m = 127 \text{ cm}^2 \Omega^{-1} \text{ mol}^{-1}$ in DMF. *UV-Vis (λ , nm) (ϵ , $M^{-1} \text{ cm}^{-1}$)* 325(3), 350(1.204), 360(3), 395(0.586), 430(0.643), 485(0.783), 540 (0.849), 620(1.109), 790(1.915), 890(1.921), 910(1.979). Color: green.

2.4.2. $[Ni_2L](NO_3)_2$ (**2**)

Anal. Calc. for $C_{18}H_{18}Ni_2N_4O_8S$: C, 38.1; H, 3.2; N, 9.9; S, 5.7. *Found:* C, 38.3; H, 3.5; N, 9.8; S, 5.8%. *Yield:* 36%. *IR (KBr, cm^{-1}):* 3316f, 3253f, 3159tf, 2935tf, 1626m, 1594m, 1547m, 1471m, 1444m, 1422m, 1380s, 1323w, 1305m, 1286m, 1270m, 1196m, 1154f, 1126f, 1063m, 1039m, 1019f, 976f, 964m, 892m, 856f, 816f, 784m, 766m, 759m, 739m, 693m, 676f, 638f, 592m, 553m. Color: green.

2.4.3. $[Ni_3(H_2L^1)_2(NO_3)_2]$ (**3**)

Anal. Calc. for $C_{36}H_{44}Ni_3N_6O_{10}S_2$: C, 45.0; H, 4.6; N, 8.7; S, 6.7. *Found:* C, 45.0; H, 4.6; N, 8.7; S, 6.6%. *Yield:* 25%. *IR (KBr, cm^{-1}):* 3277s, 3038m, 2833s, 1577s, 1526w, 1424s, 1335m, 1278m, 1082s, 1039s, 983s, 870s, 752s. $A_m = 42 \text{ cm}^2 \Omega^{-1} \text{ mol}^{-1}$ in DMF. *UV-Vis (λ , nm) (ϵ , $M^{-1} \text{ cm}^{-1}$)* 335(0.802), 360(0.865), 550(0.311), 725(0.548), 925(0.740). Color: green.

2.5. X-ray data collection, structure determination, and refinement

The details of the X-ray crystal structure solution and refinement are given in Table 1. Measurements were made on a Bruker SMART CCD Area Detector. All data were corrected for Lorentz and polarization effects. Empirical absorption correction was applied. Complex scattering factors were taken from the program package SHELXTL [13]. The structures were solved by direct methods, which revealed the position of all non-hydrogen atoms. All the structures were refined on F^2 by a full-matrix least-squares procedure using anisotropic displacement parameters for all non-hydrogen atoms [14]. All hydrogen atoms were located in their calculated positions and refined using a riding model. Molecular graphics were generated using ORTEP-3 [15].

3. Results and discussion

The acyclic Schiff bases H_2L and H_4L^1 were prepared in a good yield. The synthesis of H_2L was achieved in a one step procedure using the direct condensation of salicylaldehyde with 2-(2-aminoethylthio)ethanamine, and H_4L^1 was obtained by reducing H_2L in

Table 1Crystal data and structure refinement for $[(\text{NiL})_2]\cdot\text{CH}_3\text{OH}\cdot 4\text{H}_2\text{O}$ (**1**) and $[\text{Ni}_3(\text{H}_2\text{L}^1)_2(\text{NO}_3)_2]$ (**3**).

	(1)	(3)
Empirical formula	$\text{C}_{37}\text{H}_{48}\text{N}_4\text{O}_9\text{S}_2\text{Ni}_2$	$\text{C}_{36}\text{H}_{44}\text{N}_6\text{O}_{10}\text{S}_2\text{Ni}_3$
Formula weight	874.33	961.02
<i>T</i> (K)	293(2)	293(2)
λ (Å)	0.71073	0.71073
Crystal system	orthorhombic	monoclinic
Space group	<i>Pbcn</i>	<i>P21/c</i>
Unit cell dimensions		
<i>a</i> (Å)	13.8664(18)	11.573(4)
<i>b</i> (Å)	14.8691(19)	18.768(6)
<i>c</i> (Å)	21.014(3)	10.027(3)
β (°)		111.141(6)
<i>V</i> (Å ³)	4332.6(10)	2031.5(11)
<i>Z</i>	4	2
<i>D</i> _{calc} (Mg/m ³)	1.340	1.571
Absorption coefficient (mm ⁻¹)	1.018	1.542
<i>F</i> (000)	1832	996
Crystal size (mm)	0.34 × 0.34 × 0.23	0.20 × 0.17 × 0.10
θ range for data collection (°)	1.94–25.02	1.89–25.07
Index ranges	$-16 \leq h \leq 16, -17 \leq k \leq 17, -24 \leq l \leq 24$	$-13 \leq h \leq 13, -22 \leq k \leq 22, -11 \leq l \leq 11$
Reflections collected	30106	15498
Independent reflections	3832 (<i>R</i> _{int} = 0.0416)	3594 (<i>R</i> _{int} = 0.0612)
Completeness to theta (°)	100% (25.02)	99.9% (25.07)
Absorption correction	empirical	empirical
Maximum and minimum transmission	0.7995 and 0.7234	0.8611 and 0.7480
Refinement method	full-matrix least-squares on <i>F</i> ²	full-matrix least-squares on <i>F</i> ²
Data/restraints/parameters	3832/0/242	3594/0/267
Goodness-of-fit on <i>F</i> ²	1.100	1.053
Final <i>R</i> indices [<i>I</i> > 2σ(<i>I</i>)]	<i>R</i> ₁ = 0.0672, <i>wR</i> ₂ = 0.2205	<i>R</i> ₁ = 0.0397, <i>wR</i> ₂ = 0.0771
<i>R</i> indices (all data)	<i>R</i> ₁ = 0.0906, <i>wR</i> ₂ = 0.2586	<i>R</i> ₁ = 0.0825, <i>wR</i> ₂ = 0.0997
Largest difference in peak and hole (e Å ⁻³)	1.604 and -0.324	0.438 and -0.366

methanol with sodium borohydride. The mass spectra of the two ligands present an intense peak at *m/z* 329 and 333, respectively, corresponding to the molecular ions of the protonated ligands. The presence of phenol hydroxyl and imine moiety in the free ligand **H₂L** were confirmed by the appearance in the IR spectrum of an intense broad band centered at *ca.* 3354 cm⁻¹ (*v*_{O-H}), a strong band at 1640 cm⁻¹ *v*_{C=N} and bands of medium intensity at 1577, 1526 and 1461 cm⁻¹ (*v*_{C=C}). In the IR spectrum of the **H₄L¹** no band assignable to *v*_{C=N} was observed. This fact confirms the reduction of **H₂L**. The ¹H NMR spectra of the ligands are comparable and show the reduction of the imine group. Indeed, the signal at δ 8.4 ppm observed in the spectrum of **H₂L** corresponding to (HC=N), disappears in the spectrum **H₄L¹** while two new signal appear at δ 4.9 and 3.8 ppm, representative of -NH- and Ar-CH₂-N, respectively. The ¹³C NMR spectrum of **H₂L** shows a signal at δ 166.06 ppm which represent the carbon atom of the imine C=N group. This peak shifts to δ 46.84 ppm upon reduction of **H₂L** to **H₄L¹**. The peaks at δ 161.04 and 158.07 ppm represent the aromatic C_{ipso} of the OH of the phenol in **H₂L** and **H₄L¹** spectra, respectively.

The coordination ability of **H₂L** and **H₄L¹** towards hydrated perchlorate and nitrate salts of Ni(II) in 2:1 metal:ligand molar ratio was studied by mixing methanol solutions of the corresponding ligand and metal salts. In all cases, the complexes appear to be air stable and, except complex **2**, soluble in common organic solvents. These complexes were characterized by elemental analysis, IR and UV-Vis spectroscopy, molar conductivity and magnetic measurements, except **2** due to its low solubility in common solvents mentioned above.

The elemental analysis are in good agreement with the expected values for neutral complexes. In the IR spectra of the complexes, the C=N band shift towards lower frequency on complexation of **H₂L** by Ni(II) ion, appearing near 1620 cm⁻¹ in the spectra of **1** and **2**, suggesting an interaction between the metal and the imine nitrogen atom. The hydroxyl groups of water and methanol lattice molecules appear near 3490 cm⁻¹ for **1** [16]. From

the IR of the nitrate complex **2**, information regarding the possible bonding modes of the nitrate group was obtained. For example, the bands at 1422 and 1323 cm⁻¹ are due to *v*(N=O) (*v*₁) and *v*_{as}(NO₂) (*v*₅), respectively, of the coordinated nitrate. The *v*_s(NO₂) (*v*₂) is detected at 1029 cm⁻¹. These facts are characteristic of bidentate bridging nitrate ligands [16,17]. The separation $\Delta v = v_1 - v_5$ has been used as criterion of differentiation between mono and bidentate chelating nitrates, with Δv increasing as the coordination changes from mono to bidentate and/or bridging modes [18]. The magnitude of this separation for this complex (99 cm⁻¹) is indicative of a bidentate bridging nitrate. Also, the characteristic band near 1380 cm⁻¹, typical of non-coordinated nitrate group is observed [19]. Therefore it can be concluded the probably presence of both, coordinated and ionic nitrate, counter ions in complex **2**. The IR spectrum of the complex $[\text{Ni}_3(\text{H}_2\text{L}^1)_2(\text{NO}_3)_2]$ (**3**) exhibits bands assignable to a bidentate bridging nitrate moiety. Additional band assignable to N-H stretching vibration was observed at 3227 cm⁻¹.

The electronic spectra of the complexes **1** and **3** were recorded in freshly prepared DMF solutions. A fairly symmetrical new band is observed for **1**. This band disappears in the complex from the ligand treated with NaBH₄ in order to reduce the C=N group to a saturated moiety. Therefore, the absorption at 405 nm must be associated with the C=N chromophore coordinated to the metal ion through the nitrogen atom. An intense band was also observed at 335 nm. It was absent for the free ligand and is assigned to charge transfer between the coordinated ligand and the metal ions.

The electronic spectrum of **1** exhibits four bands at 540, 620, 790 and 910 nm, while the electronic spectrum of **3** shows three band at 550, 725 and 925 nm. These values are typical of octahedral Ni(II) complexes and they can accordingly be attributed to ³T_{2g} ← ³A_{2g}, ³T_{1g}(F) ← ³A_{2g} and ³T_{1g}(P) ← ³A_{2g} transitions [20]. These results are in agreement with the X-ray crystal structure which displays the metal ion in a distorted octahedral environment.

Molar conductivities were measured for freshly prepared solutions in DMF and after standing for 2 weeks. The conductivities increased very slightly with time for all the complexes. The conductance value of complex **1** lies in the range observed for 2:1 electrolytes ($130\text{--}170\text{ cm}^2\ \Omega^{-1}\ \text{mol}^{-1}$). For the trinuclear Ni(II) complex, **3**, the conductance is $42\text{ cm}^2\ \Omega^{-1}\ \text{mol}^{-1}$ indicative of a neutral complex in DMF solution [21].

Crystals of $[(\text{NiL})_2]\cdot\text{CH}_3\text{OH}\cdot 4\text{H}_2\text{O}$ (**1**) and $[\text{Ni}_3(\text{H}_2\text{L}^1)_2(\text{NO}_3)_2]$ (**3**) suitable for X-ray diffraction were obtained by slow evaporation of the corresponding solutions.

3.1. Crystal structure of $[(\text{NiL})_2]\cdot\text{CH}_3\text{OH}\cdot 4\text{H}_2\text{O}$ (**1**)

The molecular structure of $[(\text{NiL})_2]$ is shown in Fig. 1a together with the atomic numbering scheme adopted and selected bond lengths and angles. The compound crystallizes in the centrosymmetric space group *Pbcn*. The asymmetric unit shows half molecule as the dimer lies in a crystallographic binary axis. The structure is dinuclear, with the two nickel(II) centers joined by two phenolate groups acting as a bridge. The geometry around the metal ion can be described as slightly distorted octahedral, with a N_2SO_3 core comprised by the five donor atoms of one ligand: two amine nitrogen, one sulfur atom and the two phenolate groups (one acting as terminal and the other as bridge with the other metal ion). The sixth position is occupied by the bridging phenolate oxygen of the other ligand molecule. The equatorial plane of the octahedron is formed by $\text{N}(2)\text{--S}(1)\text{--O}(1)\text{--O}(2)\#1$ (rms 0.0631) with the Ni ion 0.0243 Å out of this plane. The axial positions are occupied respectively by one N of one amine and the O of one phenolate bridge group, $174.6(2)^\circ$ [$\text{N}(1)\text{--Ni}(1)\text{--O}(2)$].

The shortest bond distance to the nickel ion corresponds to the terminal phenolate oxygen, $\text{Ni}(1)\text{--O}(1)$, 2.024(5) Å, and the longest bond distance to the sulfur atom, $\text{Ni}(1)\text{--S}(1)$, 2.5717 Å. The amine distances, $\text{Ni}(1)\text{--N}(1)$, 2.046(7) Å and $\text{Ni}(1)\text{--N}(2)$, 2.0333(6) Å, are in the range of the bridge phenolate oxygen atoms, $\text{Ni}(1)\text{--O}(2)$, 2.050(5) Å.

The two Ni ions are separated by 3.1538 Å, a distance too long to consider an intermetallic interaction, with a bridge angle of $100.6(2)^\circ$ [$\text{Ni}(1)\text{--O}(2)\text{--Ni}(1)\#1$]. These parameters are comparable to those found for similar dinuclear nickel complexes, for example

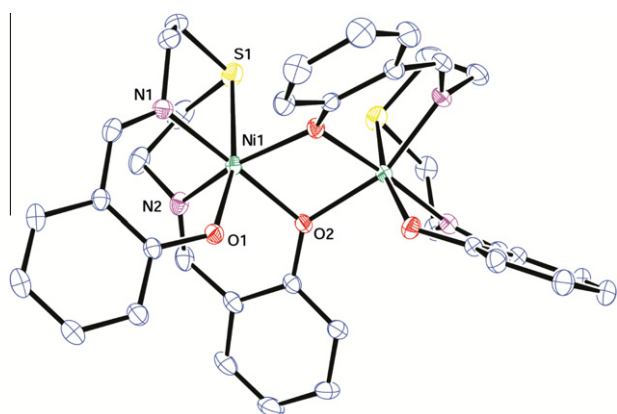


Fig. 1a. Crystal structure of $[(\text{NiL})_2]\cdot\text{CH}_3\text{OH}\cdot 4\text{H}_2\text{O}$ (**1**). Selected bond lengths (Å) and angles ($^\circ$): $\text{Ni}(1)\text{--O}(1)$ 2.024(5), $\text{Ni}(1)\text{--N}(2)$ 2.033(6), $\text{Ni}(1)\text{--N}(1)$ 2.046(7), $\text{Ni}(1)\text{--O}(2)\#1$ 2.048(5), $\text{Ni}(1)\text{--O}(2)$ 2.050(5), $\text{Ni}(1)\text{--S}(1)$ 2.572(2), $\text{O}(1)\text{--Ni}(1)\text{--N}(2)$ 95.9(3), $\text{O}(1)\text{--Ni}(1)\text{--N}(1)$ 86.7(2), $\text{N}(2)\text{--Ni}(1)\text{--N}(1)$ 97.1(3), $\text{O}(1)\text{--Ni}(1)\text{--O}(2)\#1$ 96.0(2), $\text{N}(2)\text{--Ni}(1)\text{--O}(2)\#1$ 159.3(2), $\text{N}(1)\text{--Ni}(1)\text{--O}(2)\#1$ 100.4(2), $\text{O}(1)\text{--Ni}(1)\text{--O}(2)$ 88.4(2), $\text{N}(2)\text{--Ni}(1)\text{--O}(2)$ 85.8(2), $\text{N}(1)\text{--Ni}(1)\text{--O}(2)$ 174.6(2), $\text{O}(2)\#1\text{--Ni}(1)\text{--O}(2)$ 77.7(2), $\text{O}(1)\text{--Ni}(1)\text{--S}(1)$ 166.59(15), $\text{N}(2)\text{--Ni}(1)\text{--S}(1)$ 81.1(2), $\text{N}(1)\text{--Ni}(1)\text{--S}(1)$ 80.72(18), $\text{O}(2)\#1\text{--Ni}(1)\text{--S}(1)$ 90.94(15), $\text{O}(2)\text{--Ni}(1)\text{--S}(1)$ 104.35(15). Symmetry transformations used to generate equivalent atoms: #1 $-x, y, -z + 1/2$.

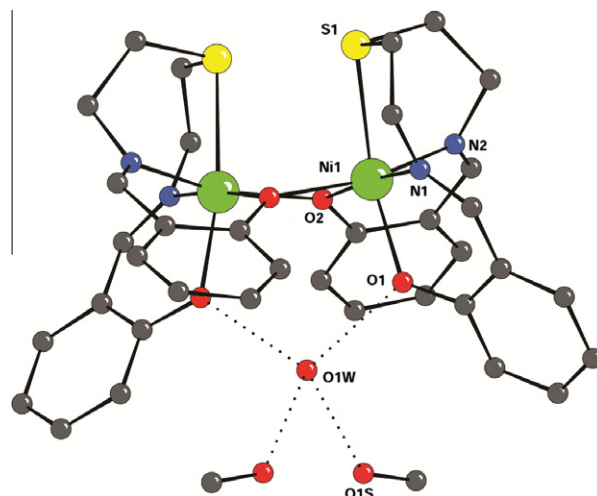


Fig. 1b. Hydrogen bond interaction of one water molecule with methanol and phenolate groups in $[(\text{NiL})_2]\cdot\text{CH}_3\text{OH}\cdot 4\text{H}_2\text{O}$ (**1**).

$[\text{Ni}(\text{dpmap})(\text{H}_2\text{O})_2(\text{ClO}_4)_2\cdot 3(\text{CH}_3)_2\text{CO}]$ (dpmap is 2-[[di(2-pyridyl)methyl](methyl)-amino] methyl]phenol) [22].

Disordered water molecules are present in the structure. O1w and O3w lies also in the crystallographic binary axis. O1w, interacts through hydrogen bonding with methanol molecules and the terminal O1 phenolate groups (Fig. 1b). [$\text{O1W}\cdots\text{O1S}$ 2.649 Å], [$\text{O1W}\cdots\text{O1}$ 2.502 Å].

3.2. Crystal structure of $[\text{Ni}_3(\text{H}_2\text{L}^1)_2(\text{NO}_3)_2]$ (**3**)

The molecular structure of the complex $[\text{Ni}_3(\text{H}_2\text{L}^1)_2(\text{NO}_3)_2]$ is illustrated in Fig. 2 together with selected bond lengths and angles. The figure shows a trinuclear centrosymmetric complex, with the three nickel ions in linear array joined by two ligands molecules through phenolate bridge groups and two bidentate nitrate moieties. The geometry about all of the Ni(II) ions can be regarded as distorted octahedral. The two terminal Ni ions are in a N_2SO_3 core, being coordinated by the donor atoms of one ligand molecule – two secondary amine nitrogen atoms, two bridge phenolate groups and the terminal sulfur atom- and one oxygen atom from a bidentate bridging nitrate moiety. Two nitrogen atoms, N(1) and N(2) and two oxygen atoms O(1) and O(2) from the ligand form the equatorial plane of the distorted octahedron (rms 0.0056) with the Ni ion 0.0445 Å out of it. Thus, the axial positions are occupied by the sulfur atom of the ligand, S(1) and the oxygen O(1N) from the bidentate bridge nitrate, [$\text{O}(1\text{N})\text{--Ni}(1)\text{--S}(1)$, $172.96(9)^\circ$]. The Ni–N distances [$\text{Ni}(1)\text{--N}(1)$, 2.095(4) Å and $\text{Ni}(1)\text{--N}(2)$, 2.086(4) Å] are comparable to those found for the octahedral complex $[\text{Ni}(\text{ampy})_2(\text{NO}_3)_2]$ (ampy is 2-aminomethylpyridine) [2.0811(11) Å] [23]. The Ni–O_{phenolate} distances [$\text{Ni}(1)\text{--O}(1)$, 2.011(3) Å and $\text{Ni}(1)\text{--O}(2)$, 2.034(3) Å] are in the order of similar complexes [24]. The nickel nitrate distance [$\text{Ni}(1)\text{--O}(1\text{N})$, 2.158(3) Å] and the longest coordination distance to the sulfur atom, [$\text{Ni}(1)\text{--S}(1)$, 2.3748(15) Å] are comparable with the values found for similar nickel octahedral complexes [25,26].

The central nickel ion, Ni(2), presents an O6 distorted octahedral environment, being coordinated by the bridging phenolate oxygen atoms of the two ligand molecules that constitutes the equatorial plane [$\text{O}(1)\text{--O}(2)\text{--O}(1)\#1\text{--O}(2)\#1$, rms 0.000] with Ni(2) seated in that plane. The axial positions are occupied by two oxygen atoms from a different bidentate bridge nitrate moiety. The Ni(2)–O_{phenolate} distances are similar, [$\text{Ni}(2)\text{--O}(2)$, 1.994(3) Å and $\text{Ni}(2)\text{--O}(1)$, 2.002(3) Å] and shorter than the Ni(2)–O_{nitrate}, 2.188(3) Å, which is comparable to those found in octahedral

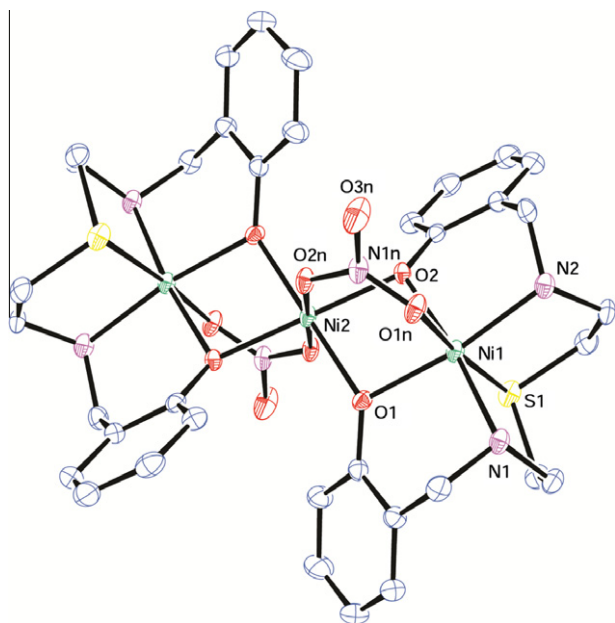


Fig. 2. Crystal structure of $[\text{Ni}_3(\text{H}_2\text{L})_2(\text{NO}_3)_2]$ (**3**). Selected bond lengths (Å) and angles ($^\circ$): Ni(1)–O(1) 2.011(3), Ni(1)–O(2) 2.034(3), Ni(1)–N(2) 2.086(4), Ni(1)–N(1) 2.095(4), Ni(1)–O(1N) 2.158(3), Ni(1)–S(1) 2.3748(15), Ni(2)–O(2)#1 1.994(3), Ni(2)–O(2) 1.994(3), Ni(2)–O(1) 2.002(3), Ni(2)–O(1)#1 2.002(3), Ni(2)–O(2N)#1 2.188(3), Ni(2)–O(2N) 2.188(3), O(1)–Ni(1)–O(2) 81.13(11), O(1)–Ni(1)–N(2) 171.61(14), O(2)–Ni(1)–N(2) 90.91(15), O(2)–Ni(1)–N(1) 172.85(14), N(2)–Ni(1)–N(1) 95.85(17), O(1)–Ni(1)–O(1N) 89.94(12), N(1)–Ni(1)–O(1N) 89.97(14), O(2)–Ni(1)–S(1) 96.00(9), N(2)–Ni(1)–S(1) 87.06(13), N(1)–Ni(1)–S(1) 86.69(11), O(1N)–Ni(1)–S(1) 172.96(9), O(2)#1–Ni(2)–O(2) 180.0(3), O(2)#1–Ni(2)–O(1) 97.66(12), O(2)–Ni(2)–O(1)#1 97.66(12), O(1)–Ni(2)–O(1)#1 180.0(2), O(2)–Ni(2)–O(2N)#1 95.98(11), O(2)#1–Ni(2)–O(2N) 95.98(11), O(2)–Ni(2)–O(2N) 84.02(11), O(1)#1–Ni(2)–O(2N) 92.82(11), O(2N)#1–Ni(2)–O(2N) 180.0(2). Symmetry transformations used to generate equivalent atoms: #1 $-x, -y, -z$.

$[\text{Ni}_2(\text{pamap})_2(\text{NO}_3)]\text{NO}_3$, (Hpamap is *N*-(2-hydroxy)benzyl-*N*-methyl-*N'*-(2-pyridyl)methyl-1,3-propanediamine) (2.188(2) Å) [29].

Few nitrate complexes of nickel, where the nitrate group adopted bidentate bridging mode of coordination were found in the literature [24,27] with respect to the monodentate or bidentate chelating mode [28–33]. The distance between Ni ions is 3.015 Å, shorter than that found for complex **1**, but also longer than can be considered an intermetallic interaction.

3.3. Magnetic properties

3.3.1. Magnetic properties of complex **1**

For the dinuclear complex, the room temperature value of χT 1.97 emu K mol^{-1} , (Fig. 3) is a little lower than those expected for two isolated Ni(II) ions (2.0 emu K mol^{-1} , $g = 2.00$) [34]. On cooling the χT decreases regularly, with a more rapid descent below 100 K, reaching a value of 0.02 emu K mol^{-1} at 2 K. This behavior clearly points to antiferromagnetic interactions being active within the molecule, with a small fraction of paramagnetic impurity accounting for the residual paramagnetism at low temperature. A satisfactory fit, shown in Fig. 3, was obtained by using the Van Vleck equation derived by the Hamiltonian $\hat{H} = -J\hat{S}_1 \cdot \hat{S}_2 + g\mu_B \mathbf{B} \cdot \mathbf{S}$ and including a small fraction of paramagnetic impurity, with best fit values $g = 2.123 \pm 0.004$, $J = -66.4 \pm 0.6 \text{ cm}^{-1}$, %imp = 1.5 ± 0.2 . Some authors have reported the magnetic behavior of phenolate bridged nickel (II) complexes. They have suggested that the phenolate group transmits an antiferromagnetic contribution [35–37]. They showed a linear relationship between exchange interaction owing the value of Ni–(O_{phenolate})₂–Ni bridge angle. The dinuclear complexes $[\text{Ni}_2(\text{L})(\text{pyridine})_2](\text{ClO}_4)_2$ (where L is

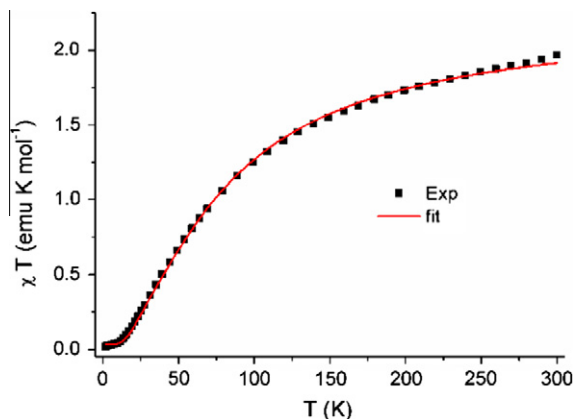


Fig. 3. Experimental (full squares) and best fit χT (emu K mol^{-1}) vs. T data (continuous line) for the dinuclear complex $[\text{Ni}(\text{L})_2] \cdot \text{CH}_3\text{OH} \cdot 4\text{H}_2\text{O}$ (**1**).

11,23-dimethyl-3,7,15,19-tetraazatricyclo [19.3.1.19,13] hexaco-*sa*-1(25),9,11,13(26),21,23-hexaene-25,26-diolate [37,38] and $[\text{Ni}_2(\text{sym-hmp})_2](\text{BPh}_4)_2 \cdot 3.5\text{DMF} \cdot 0.5(2\text{-PrOH})$ (where $[\text{H}(\text{sym-hmp})]$ is 2,6-bis[(2-hydroxyethyl)methylaminomethyl]-4-methyl-phenol [39] show a relatively stronger antiferromagnetic interaction $J = -67.1 \text{ cm}^{-1}$ and $J = -69.7 \text{ cm}^{-1}$, respectively. Thus, as complex **1** shows two bridges between the nickel atoms, with Ni–(O_{phenolate})₂–Ni angles of 100.64°, the magnitude of the antiferromagnetic interaction between the nickel centers is fully in the expected range.

3.3.2. Magnetic properties of complex **3**

Temperature dependence of the χT plots for the trinuclear Ni(II) complex **5** is shown on Fig. 4. The value of χT is 3.50 emu K mol^{-1} at 300 K and is a little higher than the spin-only value for three $S = 1$ spins with $g = 2.00$ (2.97 emu K mol^{-1}) [40] and at 2 K the χT is 0.90 emu K mol^{-1} . Upon cooling from 300 to 100 K, the χT values steadily decrease. Below 100 K, the χT values rapidly decrease with further cooling, suggesting that a dominant antiferromagnetic interaction between adjacent nickel(II) centers is operative. Indeed, the interaction between the two terminal Ni(II) cations was assumed to be negligible owing to the large distance (3.0151(9) Å) and the long path between them. The magnetic analysis was then carried out by using the isotropic spin Hamiltonian $\hat{H} = J[\hat{S}_1 \cdot \hat{S}_2 + \hat{S}_2 \cdot \hat{S}_3]$, (where the two terminal Ni are identified by \hat{S}_1 and \hat{S}_3 while the central Ni atom is named \hat{S}_2). It is interesting

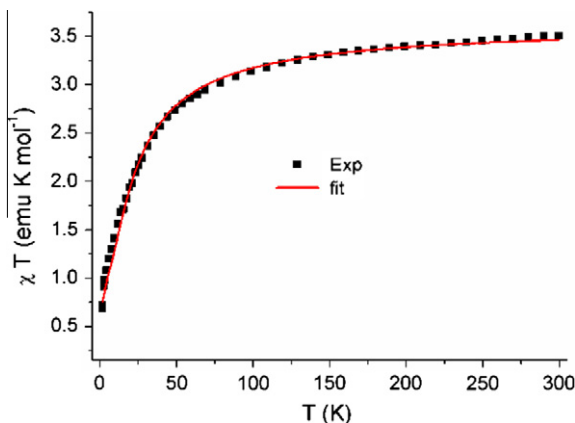


Fig. 4. Experimental (full squares) and best fit χT (emu K mol^{-1}) vs. T data (continuous line) for the dinuclear complex $[\text{Ni}_3(\text{H}_2\text{L})_2(\text{NO}_3)_2]$ (**3**).

to note that in this approach the ground state cannot be the diamagnetic one, so that a meaningful model has to include a correction to take into account possible zero field splitting effects and/or intermolecular interactions:

$$\chi = \frac{\chi_M}{1 - \chi_M \theta}$$

where χ_M is the molar magnetic susceptibility calculated on the basis of Van Vleck equation and θ is a phenomenological parameter which simulates the effect of zero field splitting effects and/or intermolecular interactions.

The best fit values obtained from the experimental data of the trinuclear complex were, $g = 2.196 \pm 0.005$, $J = -11.12 \pm 0.3 \text{ cm}^{-1}$, $\theta = -0.86 \pm 0.06 \text{ K}$.

In order to understand the exchange coupling behavior, it is important to note that the Ni(II) centers are bridged by two μ -O_{phenolate} atoms. The nature of magnetic interaction is very dependent on the bond angle M–O–M in multinuclear Ni(II) complexes [40–43]. Antiferromagnetic interaction is observed for Ni–O–Ni angles greater than 93.5° while ferromagnetic coupling is observed for angle value lower than 93.5°. In the trinuclear complex under study, bond angles of Ni1–O1–Ni2 and Ni1–O2–Ni2 are 97.4(1)° and 99.9(1)°, respectively. These values are greater than 93.5° which belong to the category of an antiferromagnetic coupling [43]. The antiferromagnetic parameters of the trinuclear complex are close to other nickel(II) complexes bridged by phenolate oxygen atoms [44].

4. Conclusion

The pentadentate salicylaldimine acyclic Schiff base ligand **H₂L** and their reduced derivative **H₄L¹** were prepared in a good yield. Starting from those ligands, dinuclear and trinuclear phenoxo bridged complexes were obtained from the reaction with nitrate and perchlorate Ni(II) salts in methanol. The ligands adopt a dianionic and pentadentate coordination nature. The complexes show the metal ion in a distorted octahedral geometry. For the trinuclear complex [Ni₃(H₂L¹)₂(NO₃)₂] (**3**), the nitrate groups act as bridge between the terminal nickel ions and the central one. Few examples of this behavior of nitrate in multinuclear nickel complexes have been reported in the literature. The magnetic data of complexes **1** and **3** indicate that antiferromagnetic coupling occurs via the phenoxo bridge.

Appendix A. Supplementary material

CCDC 868781 and 868782 contain the supplementary crystallographic data for [(NiL)₂·CH₃OH·4H₂O] (**1**) and [Ni₃(H₂L¹)₂(NO₃)₂] (**3**), respectively. These data can be obtained free of charge from The Cambridge Crystallographic Data Centre via http://www.ccdc.cam.ac.uk/data_request/cif. Supplementary data associated with this article can be found, in the online version, at <http://dx.doi.org/10.1016/j.ica.2012.09.037>.

References

- [1] P.J. Toscano, K.A. Belsky, T.C. Hsieh, T. Nicholson, J. Zubieta, *Polyhedron* 10 (1991) 977.
- [2] A.M. Guidote Jr., K. Ando, K. Terada, Y. Korusu, H. Nagao, Y. Masuyama, *Inorg. Chim. Acta* 324 (2001) 203.
- [3] S.V. Kolotilov, O. Cador, S. Golhen, O. Shvets, V.G. Ilyin, V.V. Pavlishchuk, L. Ouahab, *Inorg. Chim. Acta* 360 (2007) 1883.
- [4] S. Durmus, A. Atahan, M. Zengin, *Spectrochim. Acta, Part A* 84 (2011) 1.
- [5] Y. Fan, W. You, W. Huang, J.-L. Liu, Y.-N. Wang, *Polyhedron* 29 (2010) 1149.
- [6] H. Adam, D.E. Fenton, P.E. McHugh, *Polyhedron* 22 (2003) 75.
- [7] L. Latheef, M.R.P. Kurup, *Polyhedron* 27 (2008) 35.
- [8] M.M. Tamizh, K. Mereiter, K. Kirchner, B.R. Bhat, R. Karvembu, *Polyhedron* 28 (2009) 2157.
- [9] N. Goswami, D.M. Eichhorn, *Inorg. Chem.* 38 (1999) 4329.
- [10] E.M. Jouad, A. Riou, M. Allain, M.A. Khan, G.M. Bouet, *Polyhedron* 20 (2001) 67.
- [11] D. Fenton, P.A. Vigato, U. Casellato, R. Graziani, M. Vidali, *Inorg. Chim. Acta* 51 (1981) 195.
- [12] H.J. Banbery, F. McQuillan, T.A. Hamor, C.J. Jones, J.A. McCleverty, *Polyhedron* 8 (1989) 559.
- [13] SHELXTL version, An Integrated System for Solving and Refining Crystal Structures from Diffraction Data (Revision 5.1), Bruker AXS Ltd., WI, USA, 1997.
- [14] G.M. Sheldrick, SHELXTL-97; Program for the Refinement of Crystal Structures, University of Göttingen, Göttingen, Germany, 1997.
- [15] L.J. Farrugia, *J. Appl. Crystallogr.* 30 (1997) 565.
- [16] W.T. Carnall, S. Siegel, J.R. Ferrano, B. Tani, E. Gebert, *Inorg. Chem.* 12 (1973) 560.
- [17] J.R. Ferrano, *J. Mol. Spectrosc.* 4 (1960) 99.
- [18] K.D. Suresh, V. Alexander, *Inorg. Chim. Acta* 238 (1995) 63.
- [19] V.A.J. Aruna, V.J.J. Alexander, *J. Chem. Soc., Dalton Trans.* (1996) 867.
- [20] S. Chandra, A.K. Sharma, *Spectrochim. Acta, Part A* 72 (2009) 851.
- [21] W.J. Geary, *Coord. Chem. Rev.* 7 (1971) 81.
- [22] M.J. Prushan, D.M. Tomezsko, S. Lofland, M. Zeller, A.D. Hunter, *Inorg. Chim. Acta* 360 (2007) 2245.
- [23] S. Tanase, M. Ferbinteanu, M. Andruh, C. Mathonière, I. Strenger, G. Rombaut, *Polyhedron* 19 (2000) 1967.
- [24] S.-Y. Zhang, B. Xu, L. Zheng, W. Chen, Y. Li, W. Li, *Inorg. Chim. Acta* 367 (2011) 44.
- [25] S. Datta, D.K. Seth, R.J. Butcher, S. Bhattacharya, *Inorg. Chim. Acta* 377 (2011) 120.
- [26] P.K. Dhara, S. Sarkar, M.G.B. Drew, M. Nethaji, P. Chattopadhyay, *Polyhedron* 27 (2008) 2447.
- [27] H. Luo, J.-M. Lo, P.E. Fanwick, J.G. Stowell, M.A. Green, *Inorg. Chem.* 38 (1999) 2071.
- [28] J.L. Atwood, S.G. Bott, R.L. Vincent, *J. Cryst. Spectrosc. Res.* 20 (1990) 631.
- [29] M. Bröring, S. Prikhodovski, C.D. Brandt, *Inorg. Chim. Acta* 357 (2004) 1733.
- [30] J. Cernák, A. Pavlová, M. Dusek, K. Fejfarová, *Acta Crystallogr., Sect. C* 65 (2009) m260.
- [31] A. Mustapha, P. Duckmanton, J. Reglinski, A.R. Kennedy, *Polyhedron* 29 (2010) 2590.
- [32] J.L. Chang, Z.Y. Gao, *Acta Crystallogr., Sect. E* 67 (2011) m1506.
- [33] A. Rujiwatra, S. Yimklan, T.J. Prior, *Polyhedron* 21 (2012) 345.
- [34] J.-H. Zhou, R.-M. Cheng, Y. Song, Y.-Z. Li, Z. Yu, X.-T. Chen, X.-Z. You, *Polyhedron* 25 (2006) 2426.
- [35] Y. Aratake, M. Ohba, H. Sakiyama, M. Tadokoro, N. Matsumoto, H. Okawa, *Inorg. Chim. Acta* 212 (1993) 183.
- [36] S.K. Dey, N. Mondal, S.E. Fallah, R. Vincete, A. Escuer, X. Solans, M. Font-Bardiá, T. Matsushita, V. Gramlich, S. Mitra, *Inorg. Chem.* 43 (2004) 2427.
- [37] K.K. Nanda, R. Das, L.K. Thompson, J.N. Bridson, K. Nag, *Chem. Commun.* (1994) 1337.
- [38] K.K. Nanda, R. Das, M.J. Newlands, R. Hynes, E.J. Gabe, K. Nag, *J. Chem. Soc., Dalton Trans.* (1992) 897.
- [39] H. Sakiyama, K. Tone, M. Yamasaki, M. Mikuriya, *Inorg. Chim. Acta* 365 (2011) 183.
- [40] X.-H. Bu, M. Du, L. Zhang, D.-Z. Liao, J.-K. Tang, R.-H. Zhang, M. Shionoya, *J. Chem. Soc., Dalton Trans.* (2001) 593.
- [41] Q.-L. Wang, C. Yang, L. Qi Jr., D.Z. Liao, G.M. Yang, H.X. Ren, *J. Mol. Struct.* 892 (2008) 88.
- [42] C.J. O'Connor, *Prog. Inorg. Chem.* 29 (1982) 203.
- [43] A.K. Sharma, F. Lloret, R. Mukherjee, *Inorg. Chem.* 46 (2007) 5128.
- [44] P. Mukherjee, M.G.B. Drew, V. Tangoulis, M. Estrader, C. Diaz, A. Ghosh, *Polyhedron* 28 (2009) 2989.